A High Gain Antenna with DGS for Sub-6 GHz 5G Communications

Taiwo Olawoye[1], and Pradeep Kumar[2]
[1 & 2]Discipline of Electrical, Electronic and Computer Engineering, University of Kwazulu-Natal, King George V Avenue, Durban-4041, South Africa
Corresponding author: Taiwo Olawoye (e-mail: femi187@yahoo.com)

ABSTRACT This paper introduces the design of a high-gain wideband microstrip patch antenna (HGWMPA) for sub-6 GHz fifth generation (5G) communications. The proposed antenna integrates a novel defected ground structure (DGS) for achieving the wide bandwidth. A triangular strip is inserted into the ground plane to improve the performance of the antenna. The proposed HGWMPA also utilizes the reflective plate to concentrate the side lobes and minimize the generation of the back lobes, thereby boosting the main lobe of the radiated signal and thus increasing the gain of the antenna. The proposed HGWMPA is designed and fabricated on the FR-4 epoxy substrate and the inset feed technique is used to feed the HGWMPA. The simulation and optimization of the proposed antenna are carried out with the CST Microwave Studio Suite. The HGWMPA is compact with the substrate area of $28.03 \times 23.45\ mm^2$ and provides the maximum gain, maximum directivity and radiation efficiency of 6.21 dB, 7.56 dB and 80%, respectively. The proposed antenna operates from 4.921 GHz to 5.784 GHz, which covers the 4.9 GHz-5.8 GHz of the sub-6 GHz 5G spectrum. The antenna simulated and measured characteristics confirm that proposed high gain compact HGWMPA is suitable for sub-6 GHz wideband applications.

INDEX TERMS 5G communications, DGS, high gain, microstrip antenna, sub-6 GHz, wideband.

I. INTRODUCTION

5G technology is the technology of choice for the mobile communication systems in the foreseeable future. Its spectrum is from sub-6 GHz to the millimetre-wave frequencies. The sub-6 GHz 5G frequency spectrum has the advantages of better data rate, less fading in the rain and better coverage [1], [2]. The design of antennas for 5G operation in the sub-6 GHz frequency band significantly improves the performance as it leads to improve the overall system performance of the communication systems. The inherent advantages of microstrip patch antenna lend itself to the use of the antenna as the right choice for 5G communication systems. Microstrip antenna advantages include light weight, low cost, low profile, planar configuration, ease of conformal, suitable for arrays, etc. [3]–[6], however, the significant disadvantages of microstrip antennas are low gain, narrow bandwidth and relatively large size at low frequencies [6]–[8]. The popularity of microstrip antenna continues to soar due to improvement in design and better performance of these antennas.

Several techniques on improving the performance of microstrip patch antenna have been proposed in [7], [9]–[13]. In [12], a Frequency Selective Surface (FSS) was introduced to improve antenna gain and bandwidth, and the design achieved a gain of 17.78 dBi at 28 GHz frequency with a 9% bandwidth improvement and a radiation efficiency of 90%. In [5], a wideband antenna was designed and simulated. The results show that a bandwidth of 5.5 GHz to 7.25 GHz was achieved. In [9], FSS was used to improve the antenna bandwidth and achieve the gain of 9.4 dBi. The antenna provides the ultra-wideband (UWB) of 3.1 GHz to 18.6 GHz. It also possesses a high front-to-back lobe ratio of 10 dB over the UWB bandwidth. In [10], the DGS was introduced in antenna array, and the 2×2 array was developed with a 12 dB increase in radiation between the co-pole and the cross-pole radiation. In [13], a linear array of 4 elements was presented with the gain and directivity of 9.02 dB and 12.81 dB, respectively, following the implementation of the DGS and the reflective plate on the antenna. A single layer single probe-fed wideband antenna is presented in [14]. The rectangular patch with the cut of a U-shaped parasitic pattern around the radiating patch was designed. The resultant antenna exhibited a triband radiation at 4.82 GHz - 6.26 GHz, 5.25 GHz - 5.35 GHz and 5.725 GHz - 5.825 GHz.

In applying DGS to the design, slots are deliberately cut into the ground plane of the antenna. These slots produce an inductive and capacitive effect on the circuit. The size and position of the slot together act to tune the circuit and produce improvement on the overall performance of the antenna [15]. These slot positions and size are further optimized to maximize the performance of the circuit. The impedance added to the circuit by DGS design can be used to reduce the size of the antenna, increase its bandwidth and improve antenna gain when correctly optimized [16]–[18]. In [19], a 2.4 GHz

antenna was designed and the antenna size was reduced by implementing DGS. This resulted in an overall size reduction of 32.9% while improving the antenna gain to 8.49 dB. In [11], a 10 GHz antenna was proposed; the design used DGS to reduce the antenna size, achieving a patch reduction of 67%. In [20], a 30 GHz antenna was designed with Photonic Band Gap (PBG) utilization to improve the antenna radiation characteristics resulting in a gain of 9.39 dB over a bandwidth of 2.05 GHz. In [21], the slotted microstrip antenna was designed. The slots increase the bandwidth of the antenna producing a gain of 8 dB at 4.5 GHz frequency. In [22], the DGS was used to reduce the size of an antenna and provide enhanced operating bandwidth of 2.9 GHz to 11.4 GHz with a radiation efficiency of 88.5%.

The metamaterial split ring resonator was incorporated into the patch antenna in [23], and the resulting design achieved a resonant frequency between 4.8 GHz and 5.2 GHz. Metamaterial slip ring resonator is also used in [24], the metamaterial resonator produced 22.2% reduction in the size of the antenna, concluding that miniaturisation can be achieved by using a metamaterial slip ring resonator. In [**?**], [25], [27] microstrip patch antenna was presented where DGS technology was utilized to improve the antenna performance. A unique configuration of DGS was used in [28] to maximize the gain of the proposed antenna with a result of a maximum gain of 16.8 dB. DGS and the reflected surface were integrated into the antenna configuration of [29], resulting in a gain and directivity of 3.68 dB and 7.28 dB, respectively. In [30], a high-efficiency miniaturized antenna for the wideband application was proposed, the antenna achieved an efficiency of 78% and a gain of 5.72 dB. A frequency reconfigurable slot patch antenna was presented in [31]. The antenna used a reflector plate at its back and was able to reconfigure up to six different frequencies from 1.7 GHz to 3.5 GHz. In [32], the slotted antenna design for wideband applications was presented. The design provided the wideband of 4.4 GHz to 7.7 GHz and a gain of 6 dB, also, a stable radiation pattern was achieved. In [33], a high gain microstrip patch antenna with slotted ground plane was proposed. The antenna utilized a special lacerated C slotted ground plane and a T slotted patch to achieve a gain and directivity of 5.49 dB and 7.12 dB, respectively, while maintaining the compact size. In [34], a compact microstrip patch antenna with a U shaped slot for dual band operation was proposed. The antenna achieved the gain of 2.06 dB and 2.46 dB at two bands of frequencies with good efficiency and radiation characteristics. A new method of broadening the impedance and axial ratio (AR) bandwidths of circular polarized microstrip antennas (CPMAs) was proposed in [35], which resulted in improvements of 51.3% and 49.8% in the impedance and the axial-ratio bandwidths, respectively. In [36], authors proposed a new concept of implementing slots both in the ground plane and the radiator. The implementation achieved the multiband frequencies of 3.7 GHz, 5.7 GHz and 7.5 GHz. It achieved a size reduction of 53.5% in total volume and about 46.6% in active patch area.

For the design under consideration in this paper, we have employed DGS along with reflector surface to improve the gain and bandwidth of the antenna. The DGS applied has a slotted triangle plate attached to enhance the bandwidth of the antenna. A reflective plate was placed at the back of the antenna 2mm away from the antenna to improve the directional properties of the antenna and further improve the gain. We have achieved the bandwidth of 4.9 GHz to 5.8 GHz for the HGWMPA, which is quite considerable and makes the proposed HGWMPA suitable for sub-6 GHz 5G wireless applications. The gain and directivity of the HGWMPA are 6.21 dB and 7.56 dB, respectively with a radiation efficiency of 80%. The paper is organized in four sections: section 1 presents the introduction. The design and geometry of proposed HGWMPA are given in section 2. The measured and simulated parameters of the HGWMPA are presented in section 3. The conclusion of the work is given in section 4.

II. DESIGN AND GEOMETRY OF HGWMPA

The proposed HGWMPA utilizes the transmission model approach in calculating the dimensions of the antenna. The antenna is intended to operate at the 5.0 GHz frequency and uses the FR-4 substrate. The geometry of the proposed HGWMPA is shown in Fig. 1, Fig. 2 and Fig. 3. The top view, the ground plane, the side view and the equivalent circuit of DGS ground plane are shown in Fig. 1, Fig. 2, Fig. 3 and Fig. 4, respectively. The presented antenna employs DGS in its design to improve the properties of the antenna. A microstrip antenna without DGS produces the narrow bandwidth. The ground plane of the HGWMPA has been modified to allow for a wideband operation in the sub-6 GHz frequency band. The antenna gain has been improved by incorporating a triangle strip into the ground plane. The feeding method adopted for the proposed HGWMPA is inset feed and matched to 50Ω feeding impedance. A reflective plate is placed after optimization at 2mm away from the ground plane of the antenna to improve the antenna radiation characteristics. The reflective plate has a top copper surface etched away (i.e., single layer sheet). The copper reflective surface at the bottom of the plate is left in place, with no copper coating on the top, as shown in Fig. 3. The reflective plate serves as a reflector to concentrate the side lobes of the antenna and improve the antenna characteristics. The proposed HGWMPA operates at the sub-6 GHz frequency band of 5G communications. The proposed HGWMPA was analysed based on transmission model equations. The proposed antenna can be modelled to lumped RCL circuit as shown in Figure 4. The resistor R_1, inductors L_1, L_2 and capacitors C_1 represent the impedance introduced as a result of the patch. The triangular DGS etched to the ground plane of the antenna can be represented by inductors L_3, L_4 and capacitors C_2, C_3. While resistor R_2, inductor L_5 and capacitor C_4 represent the inductance introduced by the ground plane of the antenna.

The equivalent impedance is:

$$Z_{in} = Z_p||Z_{dgs}||Z_{ref} \quad (1)$$

where Z_p is the impedance as a result of the patch
Z_{dgs} is the impedance as a result of the DGS.
and Z_{ref} is the impedance as a result of the reflective plate.

The combined input impedance is given by:

$$Z_{in} = \frac{Z_p Z_{dgs} Z_{ref}}{Z_p Z_{dgs}} + \frac{Z_p Z_{dgs} Z_{ref}}{Z_p Z_{ref}} + \frac{Z_p Z_{dgs} Z_{ref}}{Z_{dgs} Z_{ref}} \quad (2)$$

The equivalent impedance of the patch can be determined by:

$$Z_p = R_1 + j\omega L_1 + j\omega L_2 + \frac{1}{j\omega C_1} \quad (3)$$

The equivalent impedance of the triangular DGS can be determined by:

$$Z_{dgs} = j\omega L_3 + j\omega L_4 + \frac{1}{j\omega C_2} + \frac{1}{j\omega C_3} \quad (4)$$

The equivalent impedance of the reflective plate can be determined by:

$$Z_{ref} = R_2 + j\omega L_5 + \frac{1}{j\omega C_4} \quad (5)$$

.

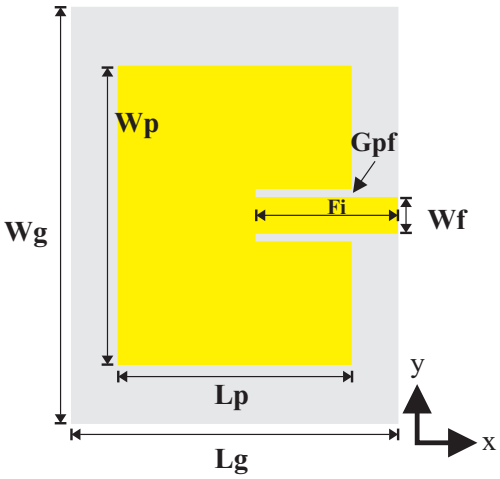

FIGURE 1. Top view of the HGWMPA.

From the transmission line model equations in [3], the width of the rectangular patch is given in equation (6):

$$W = \frac{c}{2f_r}\sqrt{\frac{2}{\varepsilon_r + 1}} \quad (6)$$

where c is the speed of the light, f_r is the resonant frequency, and ε_r is the dielectric constant of the substrate. The effective dielectric constant of the substrate due to the fringing effect is given by [3]:

$$\varepsilon_{reff} = \frac{\varepsilon_r + 1}{2} + \frac{\varepsilon_r - 1}{2\sqrt{1 + \frac{12h}{W}}} \quad (7)$$

Using equation (8) [3], the actual length of the patch is calculated.

$$L = L_{eff} - 2\Delta L = \frac{c}{2f_r\sqrt{\varepsilon_{reff}}} - 2\Delta L \quad (8)$$

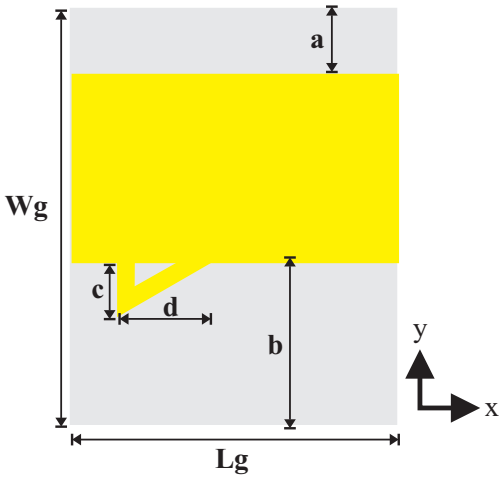

FIGURE 2. Ground plane of the HGWMPA.

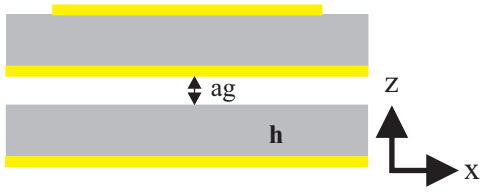

FIGURE 3. Side view of the HGWMPA.

ΔL in equation (9) is the change in length due to fringing effect and from [3], ΔL is given by:

$$\Delta L = \frac{h(0.412)\left((\varepsilon_{reff} + 0.3)\left(\frac{W}{h} + 0.264\right)\right)}{(\varepsilon_{reff} - 0.258)\left(\frac{W}{h} + 0.8\right)} \quad (9)$$

Where h is the substrate thickness or height. For this design, we have resonant frequency $f_r = 5\,GHz$, $h = 1.6\,mm$, and the dielectric constant ε_r= 4.3 with the loss tangent (tan δ) of 0.02. Table 1 shows the optimized dimensions of the HGWMPA.

III. RESULTS AND DISCUSSIONS

This antenna is designed on a lossy FR-4 substrate with a loss tangent (tan δ) of 0.02. FR-4 is readily available and cheap. The lossy nature of the substrate does not adversely affect the performance of the antenna. The simulation is performed with the commercially available EM software i.e. CST Studio Suite. The results of various steps in design evolution of the

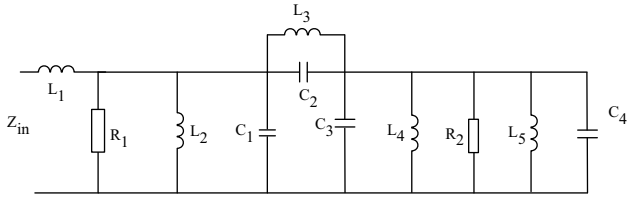

FIGURE 4. Equivalent circuit.

TABLE 1. Dimensions of the proposed HGWMPA

S. No.	Parameters	Dimensions (mm)
1	Wg	28.03
2	Lg	23.45
3	Wp	18.43
4	Lp	13.85
5	h	1.6
6	Fi	5.2
7	Wf	3.04
8	Gpf	0.1
9	ag	2
10	a	5
11	b	10
12	c	4.5
13	d	5.6

HGWMPA are analyzed. The antenna with the DGS only i.e. without reflector plate is named as antenna with DGS (ADGS) and the antenna without DGS and reflective plate is named as the Plane Antenna (PA). The complete antenna (CA) i.e. HGWMPA is with the DGS and the reflective plate. The HGWMPA achieves better radiation properties when compared to ADGS and PA. After simulation, optimization and adjusting the position of a reflective plate placed at the back of the HGWMPA, the reflective plate was placed at 2 mm, where it achieves the optimum performance. The reflective plate utilizes a single sided FR-4 substrate. The thickness of the plate is indicated in the Table 1. The plate helps to focus the antenna radiation by reducing the side-lobes and back lobe of the antenna. Optimization of the design results in a wide bandwidth and the novel triangular plate on the ground plane improves the gain of the antenna. The antenna without the triangular slot yield a narrow band antenna. The incorporation and optimization of the triangular slot on the ground plane further enhances the bandwidth of the antenna. Table 1 shows the optimized dimension of the antenna including the triangular plate incorporated into the design to achieve a good response. Fig. 5 shows the simulated reflection coefficient of the three configurations. The minimum reflection coefficient of PA, ADGS and HGWMPA are -36 dB, -26 dB and -18 dB, respectively. It is clear that the bandwidth of the proposed HGWMPA is from 4.921 GHz to 5.784 GHz, which is a wideband in the sub-6 GHz frequencies.

Fig. 6 and Fig. 7 show the simulated normalized patterns at 4.8 GHz in $phi = 90deg.plane$ and in $phi = 0deg.plane$, respectively. Fig. 8 and Fig. 9 show the simulated normalized patterns at 5.4 GHz for $phi = 90deg.$ and $phi = 0deg.$ while Fig. 10 and Fig. 11 show the simulated normalized pattern plot at 5.8 GHz for $phi = 90deg.plane$ and $phi = 0deg.plane$, respectively. These patterns show that the HGWMPA has the best directional characteristics. The HGWMPA has good properties in both i.e. $phi = 0deg.plane$ and and $phi = 90deg.plane$ over the three frequencies. ADGS exhibits bad directional properties as its back lobe is significant. PA, on the other hand, has better properties

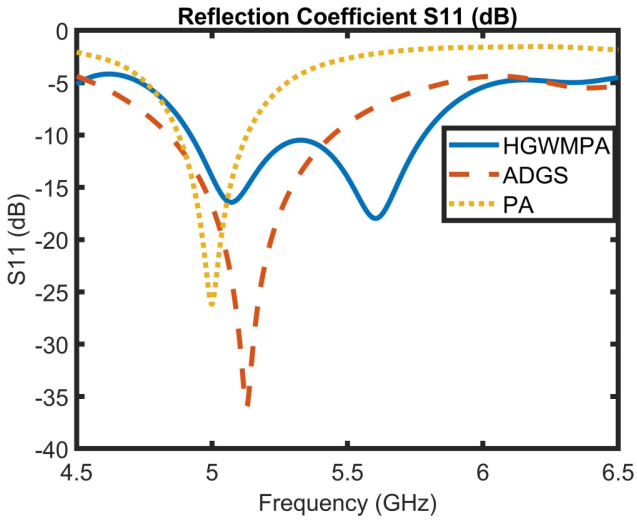

FIGURE 5. Reflection coefficient of PA, ADGS and HGWMPA.

at $phi = 90deg.plane$ and $phi = 0deg.plane$ close to the behavior of HGWMPA at all the three frequencies tested but exhibit a narrow band. This makes HGWMPA to have the best radiation properties among the three antennas and hence the HGWMPA is fabricated and tested. Fig. 12 shows the simulated gain of the PA, ADGS and HGWMPA from 4.8 GHz to 5.8 GHz. The proposed HGWMPA has the highest gain over the entire frequency range. ADGS has low values of gain because of the partial ground plane at the bottom of the antenna. Fig. 13 shows the simulated total efficiency of the PA, ADGS and HGWMPA over the same frequency range, i.e., 4.8 GHz to 5.8 GHz. HGWMPA has the highest total efficiency as compared to the ADGS and PA. The proposed HGWMPA has a better performance as compared to PA and ADGS. The HGWMPA is fabricated and measured. Fig. 14 and Fig. 15 show the top view and the bottom view of the fabricated HGWMPA, respectively. The HGWMPA is compact with the good radiation properties. The input characteristics and radiation characteristics of the fabricated HGWMPA are measured. The measurement of the input characteristics of the HGWMPA is performed using the Rohde & Schwarz 13.6 GHz network analyzer. The measurement of the radiation characteristics of the HGWMPA is performed in the anechoic chamber. The HGWMPA is used as the transmitter and the horn antenna is used as the receiver. Fig. 16 shows the reflection coefficient of the simulated and measured HGWMPA. The curve shows the wideband property of the antenna but with a much lower S11 dip at $-26\ dB$ which indicates the better reflection coefficient as against the simulated antenna of $-19\ dB$. The measured voltage standing wave ratio of the antenna (VSWR) as expected has a good result close to 1 at 1.11 which is better compared to the simulated value at 1.29. Fig. 17 through Fig. 18 show the normalized radiation

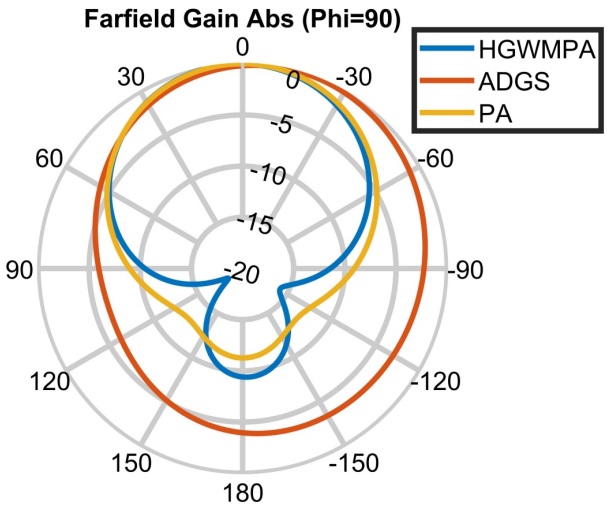

FIGURE 6. Normalized radiation patterns of the PA, ADGS and HGWMPA at 4.8 GHz (Phi=90 deg. plane).

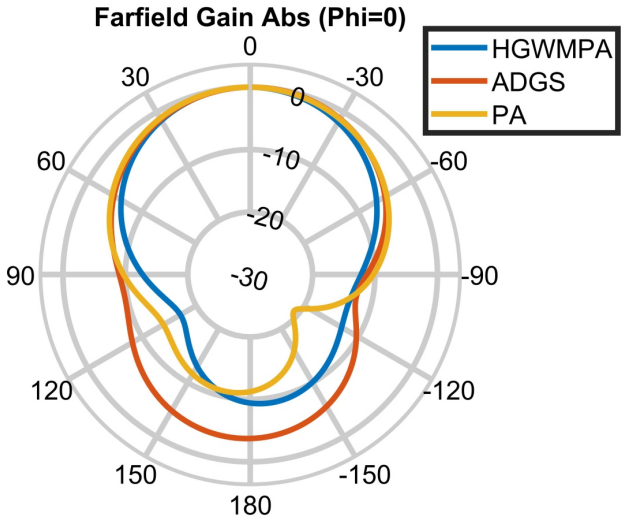

FIGURE 7. Normalized radiation patterns of the PA, ADGS and HGWMPA at 4.8 GHz (Phi=0 deg. plane).

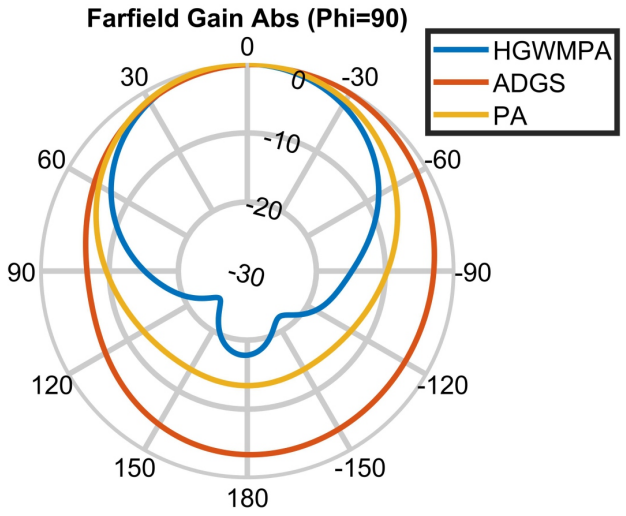

FIGURE 8. Normalized radiation patterns of the PA, ADGS and HGWMPA at 5.4 GHz (Phi=90 deg. plane).

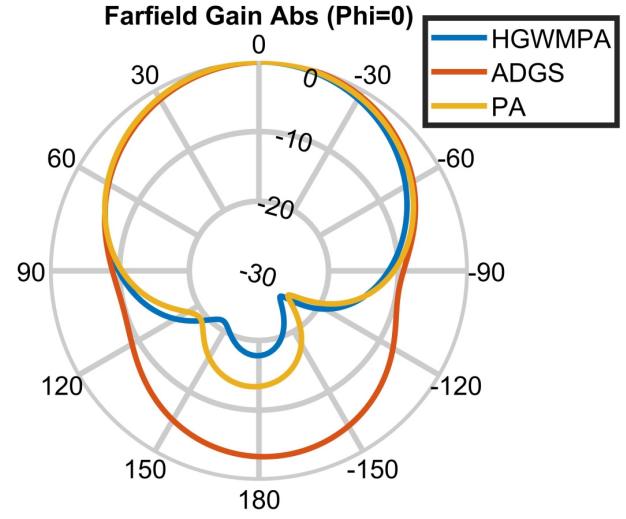

FIGURE 9. Normalized radiation patterns of the PA, ADGS and HGWMPA at 5.4 GHz (Phi=0 deg. plane).

patterns of the HGWMPA at 5.4 GHz and 5.8 GHz in both i.e. $Phi = 90deg.$ and $Phi = 0deg.$ planes. The simulated and measured patterns show good agreement in both planes.

Table 2 shows the main lobe direction and beamwidth of the PA, ADGS and HGWMPA at various frequencies. From the table, it is clear that the main lobe direction for HGWMPA is better than ADGS and PA with the maximum deviation of 2 degrees. The 3 dB beamwidth for HGWMPA is fine over the same frequencies. Table 3 shows the simulated maximum gain, maximum directivity and efficiency of the PA, ADGS and HGWMPA. It is clear from the table that the gain and directivity for HGWMPA is highest while that of ADGS is lowest partly because of the partial ground plane. The total efficiency and radiation efficiency of HGWMPA is also better over the entire bandwidth. Table 4 shows the comparison of the proposed HGWMSA with the other single/multiband sub-6 GHz antennas in literature. From this table, it can be observed that the proposed low cost HGWMPA is compact in size and provides high gain and wide bandwidth.

IV. CONCLUSION

A high gain wideband compact rectangular microstrip patch antenna for sub-6 GHz 5G applications has been presented. The simulation and optimization have been done using CST Studio Suite which is a commercial EM tool software. The

TABLE 2. Main lobe direction and 3 dB beamwidth of PA, ADGS and HGWMPA/CA at various frequencies

Frequency (GHz)	Main lobe direction ($phi = 0$ deg plane) (in degrees)			Main lobe direction ($phi = 90$ deg plane) (in degrees)			3 dB beam-width ($phi =$ 0 deg) (in degrees)			3 dB beam-width ($phi =$ 90 deg) (in degrees)		
	CA	ADGS	PA	CA	ADGS	PA	CA	ADGS	PA	CA	ADGS	PA
4.8	1.0	2.0	0.0	1.0	16.0	0.0	80.8	93.0	96.0	88.3	167.8	92.5
4.9	1.0	2.0	0.0	1.0	15.0	0.0	82.7	93.0	95.6	87.3	161.7	91.6
5.0	0.0	2.0	0.0	1.0	15.0	0.0	84.5	93.1	95.1	85.3	155.9	90.7
5.1	0.0	3.0	0.0	1.0	14.0	0.0	86.0	93.1	94.7	82.6	150.0	89.8
5.2	0.0	3.0	1.0	1.0	13.0	0.0	87.2	93.2	94.4	79.4	144.6	89.0
5.3	0.0	4.0	1.0	2.0	12.0	0.0	87.8	93.4	94.0	76.3	139.9	88.2
5.4	0.0	5.0	2.0	1.0	11.0	0.0	87.9	93.5	93.8	74.0	135.8	87.5
5.5	0.0	6.0	2.0	1.0	10.0	0.0	87.6	93.5	93.5	72.8	131.7	86.9
5.6	1.0	8.0	3.0	1.0	9.0	0.0	87.3	93.7	93.3	72.4	127.7	86.3
5.7	1.0	9.0	3.0	1.0	7.0	0.0	87.1	93.8	93.1	72.5	124.0	86.0
5.8	2.0	11.0	4.0	2.0	5.0	0.0	87.2	94.0	93.0	73.0	120.4	86.0

TABLE 3. Gain, directivity and efficiencies of PA, ADGS and HGWMPA/CA at various frequencies

Frequency (GHz)	Max. Gain (dB)			Max. Directivity (dB)			Total Efficiency (dB)			Radiation Efficiency (dB)		
	CA	ADGS	PA	CA	ADGS	PA	CA	ADGS	PA	CA	ADGS	PA
4.8	5.89	3.07	4.13	7.08	4.16	6.28	-2.25	-1.62	-3.24	-1.18	-1.09	-2.15
4.9	5.96	3.08	4.23	7.16	4.19	6.34	-1.70	-1.38	-2.43	-1.21	-1.11	-2.10
5.0	6.00	3.06	4.27	7.22	4.21	6.39	-1.36	-1.24	-2.17	-1.22	-1.14	-2.12
5.1	6.04	3.01	4.28	7.28	4.21	6.45	-1.30	-1.21	-2.42	-1.25	-1.20	-2.16
5.2	6.10	2.94	4.25	7.37	4.21	6.50	-1.43	-1.29	-3.08	-1.27	-1.27	-2.25
5.3	6.17	2.85	4.12	7.47	4.21	6.53	-1.57	-1.46	-4.02	-1.30	-1.36	-2.41
5.4	6.21	2.75	3.87	7.56	4.20	6.56	-1.60	-1.71	-5.06	-1.35	-1.46	-2.69
5.5	6.18	2.61	3.55	7.60	4.18	6.57	-1.53	-2.04	-6.05	-1.42	-1.58	-3.03
5.6	6.05	2.44	3.20	7.59	4.17	6.58	-1.56	-2.42	-6.97	-1.54	-1.72	-3.38
5.7	5.84	2.26	2.83	7.53	4.15	6.58	-1.80	-2.84	-7.82	-1.69	-1.89	-3.75
5.8	5.31	2.06	2.38	7.44	4.13	6.54	-2.29	-3.27	-8.63	-1.91	-2.07	-4.17

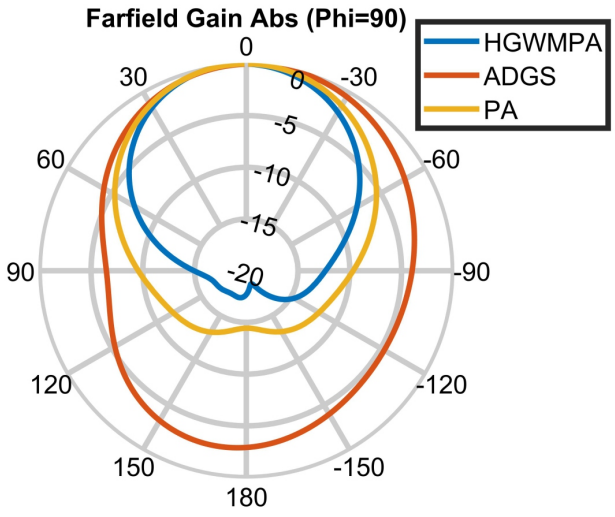

FIGURE 10. Normalized radiation patterns of the PA, ADGS and HGWMPA at 5.8 GHz (Phi=90 deg. plane).

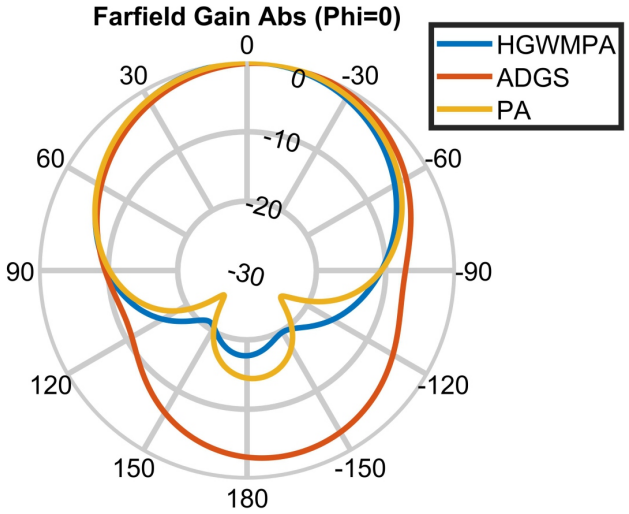

FIGURE 11. Normalized radiation patterns of the PA, ADGS and HGWMPA at 5.8 GHz (Phi=0 deg. plane).

antenna provides the maximum gain and maximum directivity of 6.21 dB and 7.29 dB, respectively over a wideband of 4.9 GHz to 5.8 GHz. The reflective plate along with DGS is utilized to improve the performance of the antenna. The size of the antenna remains compact with the area of 28.03 mm $\times$ 23.45 mm. The HGWMPA is fabricated and measured. The simulated and measured results show good agreement. The antenna parameters confirm that the proposed compact HGWMPA is suitable for sub-6 GHz 5G communications.

TABLE 4. Comparison of the proposed HGWMPA with existing antennas

Ref.	Antenna size (mm^2)	Substrate (ϵ_r)	Bandwidth	Gain(dB/dBi)	App.
[14]	44.6 × 51.3	FR4(4.4)	4.75-6.22 GHz	7.73	SBS65GA
[33]	28.0289 × 23.4493	FR4 (4.3)	4.775-5.049 GHz	5.49	SBS65GA
[36]	24.8 × 30	FR4(4.4)	5.64-5.96 GHz for 5.7 GHz band	1.13 dB at 5.6 GHz	TBXS65GA
[37]	23.88 × 23.88	FR4 (4.4)	3.2-5.34 GHz	2.75	SBS65GA
[38]	24 × 24	Rogers 4700 (2.5)	3.68-3.89 for 3.7 GHz band	4.3 (at 3.7 GHz)	DBS65GA
[39]	35 × 57.4	FR4 (4.4)	5.15-5.35 GHz(ap.) for 5.2 GHz band	5.9 at 5.2 GHz	TBS65GA
[40]	110 × 110 (ap.)	Air(1)	5.137-5.853 GHz	5.18 at 5.85 GHz	DBS65GA
[41]	45 × 40	Rogers 5880(2.3)	4.58-5.8 GHz for 5.5 GHz band	3.76 dB for 5.5 GHz band	TBKS65GA
[42]	53.6 × 52	FR4(4.3)	5.75-6 GHz for third band	0.416 for third band	TBS65GA
[43]	40 × 28 (ap.)	FR4(4.4)	3.3-4 GHz	2.5	SBS65GA
[44]	40 × 30	FR4	3-5.64 GHz	3.22	SBS65GA
[45]	54.5 × 22	2.2	2.6-6 GHz	9	SBS65GA
[46]	0.58 × 0.23	2.5	2.3-5.2 GHz	3	SBS65GA
[47]	40 × 40	FR4(4.4)	4.89-7.43 GHz	4	SBCS65GA
Prop.	28.03 × 23.45	FR4(4.3)	4.921-5.784 GHz	6.21	SBS65GA

Ap.-Approximate, App.-Applications, DBS65GA-Dual band sub-6 GHz 5G applications, Prop.-Proposed, Ref.-Reference, SBS65GA-Single band sub-6 GHz 5G applications, SBCS65GA-Single band C-band and sub-6 GHz 5G applications, TBS65GA-Triple band sub-6 GHz 5G applications, TBKS65GA-Triple band Ka band and sub-6 GHz 5G applications, TBXS65GA-Triple band X-band and sub-6 GHz 5G applications.

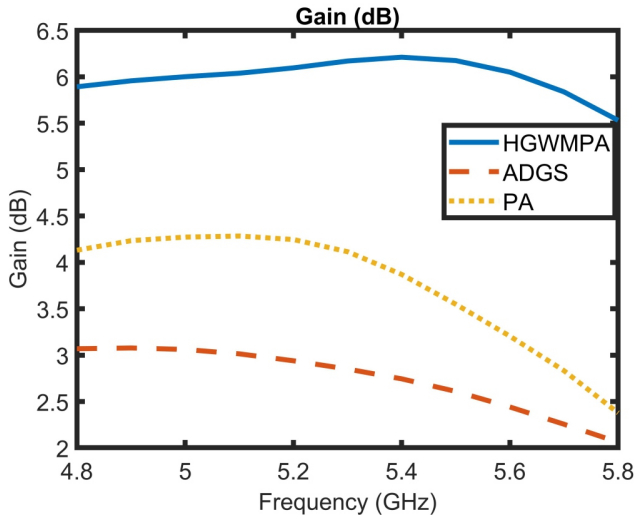

FIGURE 12. Gain of the PA, ADGS and HGWMPA.

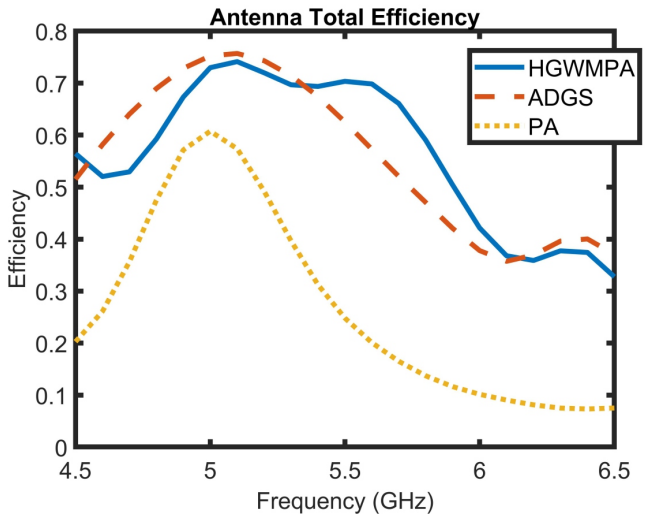

FIGURE 13. Total efficiency of the PA, ADGS and HGWMPA.

REFERENCES

[1] D. Schnaufer, B. Peterson, "Realizing 5G sub-6-GHz massive MIMO using GaN," Microwave. & RF, pp. 4–8, 2018.

[2] E. O'Connell et al., "Challenges associated with implementing 5G in manufacturing," Telcom, Vol. 1, no. 1, pp. 48-67, 2020.

[3] C. A. Balanis, Antenna Theory Analysis and Design, Fourth edition., Hoboken, New Jersey, John Wiley & Sons, Inc., 2016.

[4] A. Taggu et al., "A dual band omni-directional antenna for WAVE and Wi-Fi," 2017 2nd International Conference on Communication Systems, Computing and IT Applications (CSCITA),IEEE, pp. 1-4, 2017.

[5] D. Nataraj, G. Karunakar, "Design and research of miniaturized microstrip slot with and without defected ground structure," Int. J. Recent Technol. Eng., vol. 8, no. 2, pp. 391–398, 2019.

[6] Y. Liu et al., "Some recent developments of microstrip antenna," International Journal of Antennas and Propagation, vol. 2012, 2012.

[7] R. Garg et al., Microstrip Antenna Design Handbook, Artech house, 2001.

[8] A. Pandey, Practical Microstrip and Printed Antenna Design, Artech House, 2019.

[9] R. Mondal et al., "Compact ultra-wideband antenna: improvement of gain and FBR across the entire bandwidth using FSS," IET Microwaves,

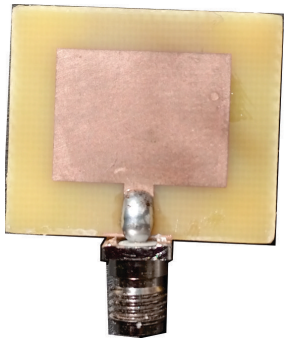

FIGURE 14. Top view of the fabricated HGWMPA.

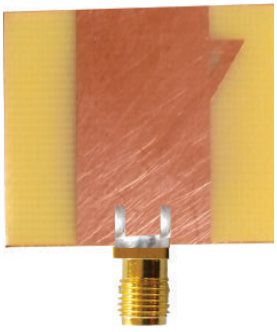

FIGURE 15. Ground plane of the fabricated HGWMPA.

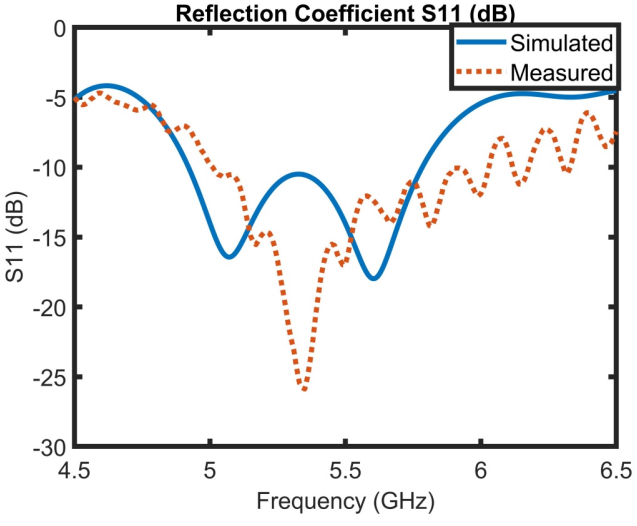

FIGURE 16. Simulated and measured reflection coefficient of the HGWMPA.

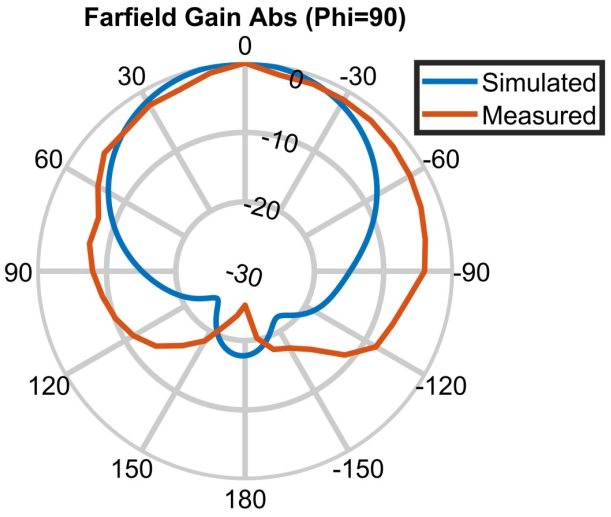

FIGURE 17. Simulated and measured normalized radiation patterns of the HGWMPA at 5.4 GHz (Phi=90 deg. plane).

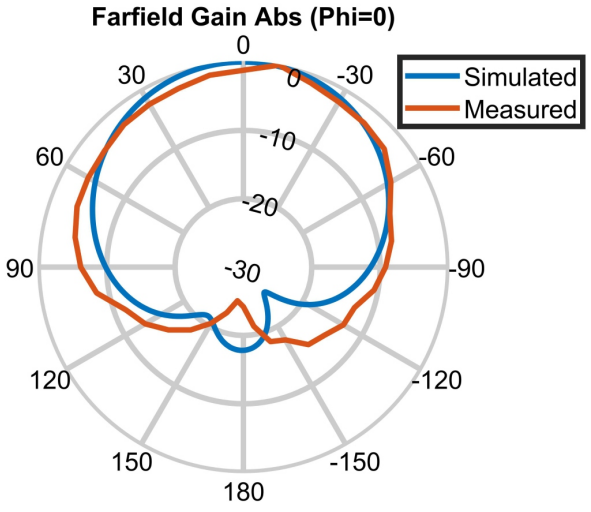

FIGURE 18. Simulated and measured normalized radiation patterns of the HGWMPA at 5.4 GHz (Phi=0 deg. plane).

Antennas & Propagation, vol. 14, no. 1, pp. 66-74, 2019.
[10] C. Kumar et al., "Defected ground structure integrated microstrip array antenna for improved radiation properties," IEEE Antennas and Wireless Propagation Letters, vol. 16, pp. 310-312, 2016.
[11] G. P. Mishra et al., "Direct and electromagnetically coupled compact microstrip antenna design with modified fractal DGS," International Journal of RF and Microwave Computer-Aided Engineering, vol. 29, no. 10, e21887, 2019.
[12] M. Asaadi et al., "High gain and wideband high dense dielectric patch antenna using FSS superstrate for millimetre-wave applications," IEEE Access, vol. 6, pp. 38243-38250, 2018.
[13] B. W. Ngobese, P. Kumar, "A high gain microstrip patch array for 5 GHz WLAN applications," Advanced Electromagnetics, vol. 7, no. 3, pp. 93-98, 2018.
[14] H. X. Lu et al. "Design and analysis of wideband U-slot patch antenna with U-shaped parasitic elements," International Journal of RF and Microwave Computer-Aided Engineering, vol. 28, no. 2, e21202, 2018.
[15] R. H. Thaher, Z. S. Jamel, "New design of dual-band microstrip antenna for

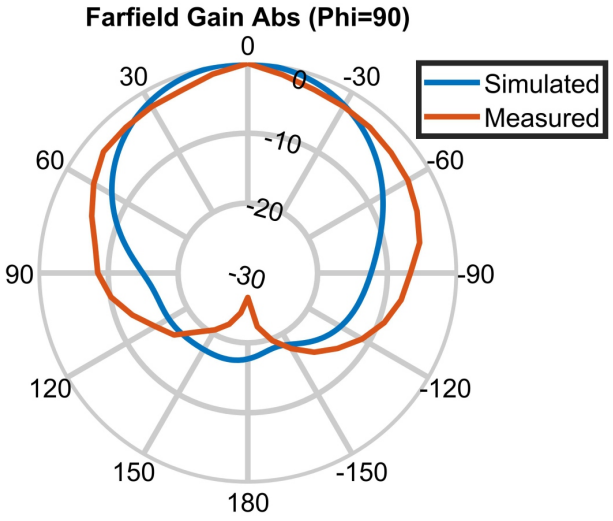

FIGURE 19. Simulated and measured normalized radiation patterns of the HGWMPA at 5.8 GHz (Phi=90 deg. plane).

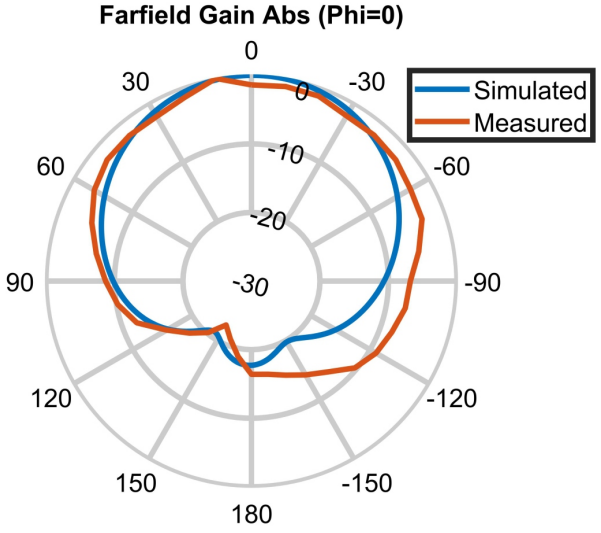

FIGURE 20. Simulated and measured normalized radiation patterns of the HGWMPA at 5.8 GHz (Phi=0 deg. plane).

Wi-Max and WLAN applications," 2018 1st International Scientific Conference of Engineering Sciences-3rd Scientific Conference of Engineering Science (ISCES), IEEE, pp. 131-134, 2018.

[16] B. Guan, Z. Zhang, "An ultra broadband antenna (UWB) loaded with defected ground structure (DGS)," 2011 International Conference on Electronics, Communications and Control (ICECC), IEEE, pp. 1872-1874, 2011.

[17] R. Hosono et al., "A broadband microstrip array antenna with rectangular waveguide mode transition at millimetre-wave band," 2017 IEEE International Symposium on Antennas and Propagation & USNC/URSI National Radio Science Meeting, IEEE, pp. 2563-2564, 2017.

[18] C. Han et al., "A dual-band millimetre-wave antenna for 5G mobile applications," 2019 IEEE International Symposium on Antennas and Propagation and USNC-URSI Radio Science Meeting, IEEE, pp. 1083-1084, 2019.

[19] R. V. Prasad et al., "A novel fractal slot DGS microstrip antenna for Wi-Fi application," 2018 IEEE Indian Conference on Antennas and Propagation (InCAP), IEEE, pp. 1-4, 2018.

[20] A. Zaidi et al., "High gain microstrip patch antenna, with PBG substrate and PBG cover, for millimetre wave applications," 2018 4th International Conference on Optimization and Applications (ICOA), IEEE, pp. 1-6, 2018.

[21] G. Immadi, G. et al., "Design of microstrip patch antenna for WLAN applications using Back to Back connection of Two E-Shapes," International Journal of Engineering Research and Applications, vol. 2, no. 3, pp. 319-323, 2012.

[22] D. Venkatachalam, M. Govindasamy, "A miniaturized planar antenna with defective ground structure for UWB applications," IEICE Electronics Express, vol. 16, no. 14, 20190242, 2019.

[23] P. Bora, C. Paul, "Metamaterial loaded CSRR based antenna for WLAN and IOT band applications," Int. J. Sci. Technol. Res., vol. 8, no. 9, pp. 2060–2065, 2019.

[24] R. Li et al., "Design of a miniaturized antenna based on split ring resonators for 5G wireless communications," 2019 Cross Strait Quad-Regional Radio Science and Wireless Technology Conference (CSQRWC), IEEE, pp. 1-4, 2019.

[25] P. Kumar, J. L. Masa-Campos, "Dual Polarized Microstrip Patch Antennas for Ultra Wideband Applications," Microwave and Optical Technology Letters, vol. 56, no. 9, pp. 2174-2179, 2014.

[26] P. Kumar, "Design of low cross-polarized patch antenna for ultra-wideband applications," International Journal on Communication Antenna and Propagation, vol. 7, no. 4, pp. 265-270, 2017.

[27] M. Mabaso, P. Kumar, "A microstrip patch antenna with defected ground structure for triple band wireless communications," Journal of Communications, vol. 14, no. 8, pp. 684-688, 2019.

[28] H. Attia et al. "Wideband and high-gain millimetre-wave antenna based on FSS Fabry–Perot cavity," IEEE Transactions on Antennas and Propagation, vol. 65, no. 10, pp. 5589-5594, 2017.

[29] N. L. Nhlengethwa, P. Kumar, "Microstrip patch antenna with enhanced gain for 2.4 GHz wireless local area network applications," Micro-Electronics and Telecommunication Engineering, pp. 583–591, 2020.

[30] H. Davoudabadifarahani, B. Ghalamkari, "High efficiency miniaturized microstrip patch antenna for wideband terahertz communications applications," Optik, vol. 194, 163118, 2019.

[31] H. A. Majid et al., "Frequency reconfigurable microstrip patch-slot antenna with directional radiation pattern," Progress In Electromagnetics Research, vol. 144, pp. 319-328, 2014.

[32] N. Rasool et al., "A wideband circularly polarized slot antenna with antipodal strips for WLAN and C-band applications," International Journal of RF and Microwave Computer-Aided Engineering, vol. 29, no. 11, e21945, 2019.

[33] T. O. Olawoye, P. Kumar, "A high gain microstrip patch antenna with slotted ground plane for sub-6 GHz 5G communications," 2020 International Conference on Artificial Intelligence, Big Data, Computing and Data Communication Systems (icABCD), IEEE, pp. 1-6, 2020.

[34] J. Ashish, A. P. Rao, "Design and implementation of compact dual band U-slot microstrip antenna for 2.4 GHz WLAN and 3.5 GHz WiMAX applications," 2019 International Conference on Smart Systems and Inventive Technology (ICSSIT), IEEE, pp. 1084-1086, 2019.

[35] Z. B. Deng et al., "A new method for broadening bandwidths of circular polarized microstrip antennas by using DGS & parasitic split-ring resonators," Progress In Electromagnetics Research, vol. 136, pp. 739–751, 2013.

[36] T. Ali et al., "A miniaturized slotted ground structure UWB antenna for multiband applications," Microwave and Optical Technology Letters Wiley Online Library, vol. 60, no. 8, pp. 2060-2068, 2018.

[37] A. Kapoor et al., "Wideband miniaturized patch radiator for sub-6GHz 5G devices", Heliyon, vol. 7, pp. 1-10, 2021.

[38] B. R. Swain and A. K. Sharma, "An investigation of dual-band dual-square ring based microstrip antenna for WiFi/WLAN and 5G-NR wireless applications," Progress in Electromagnetic Research M, vol. 86, pp. 17-26, 2019.

[39] M. Chakraborty et al., "High performance DGS integrated compact antenna for 2.4/5.2/5.8 GHz WLAN band," Radioengineering, vol. 26, no. 1, pp. 71-77, 2017.

[40] F. Meng and S. Sharma, "A single feed dual-band (2.4 GHz/5 GHz) miniaturized patch antenna for wireless local area network (WLAN) communications," Journal of Electromagnetic Waves and Applications, vol. 30, no. 18, pp. 2390-2401, 2016.

[41] M. E. Yassin et al., "Single-fed 4G/5G multiband 2.4/5.5/28 GHz antenna," IET Microwaves, Antennas & Propagation, vol. 13, no. 3, pp. 286-190, 2018.

[42] N. L. Nhlengethwa, P. Kumar, "Fractal microstrip patch antennas for dual-band and triple-band wireless applications," Int. J. on Smart Sensing and Int. Systems, vol. 14, pp. 1-9, 2021.
[43] A. Kapoor et al., Compact wideband-printed antenna for sub-6GHz fifth-generation applications, Int. J. on Smart Sensing and Int. Systems, vol. 13, pp. 1-10, 2020.
[44] P. Jha et al., "Wideband sub-6 GHz micro-strip antenna: design and fabrication," Lecture Notes in Electrical Engineering, vol. 721, 2021.
[45] J Guo et al., "Compact broadband crescent moon-shape patch-pair antenna," IEEE Antennas and Wireless Propagation Letters, vol. 10, pp. 435-437, 2011.
[46] X. Tang et al., "Ultra-wideband patch antenna for sub-6 GHz communications," International Workshop on Electromagnetics (iWEM), pp. 1-3, 2019.
[47] P. Pathak and P. K. Singhal, "Compact broadband monopole antenna for C band applications," Advanced Electromagnetics, vol. 7, no. 5, pp. 118-123, 2018.